




## ORIGINAL ARTICLE

# Foveal changes in aquaporin-4 antibody seropositive neuromyelitis optica spectrum disorder are independent of optic neuritis and not overtly progressive

Adriana Roca-Fernández<sup>1,2</sup>  | Frederike Cosima Oertel<sup>3,4</sup> | Tianrong Yeo<sup>5,6</sup> | Seyedamirhosein Motamedi<sup>3,4</sup> | Fay Probert<sup>5</sup> | Matthew J. Craner<sup>1</sup> | Jaime Sastre-Garriga<sup>2</sup>  | Hanna G. Zimmermann<sup>3,4</sup> | Susanna Assejer<sup>3,4</sup>  | Joseph Kuchling<sup>3,4,7,8</sup> | Judith Bellmann-Strobl<sup>3,4</sup> | Klemens Ruprecht<sup>7</sup> | Maria Isabel Leite<sup>1</sup> | Friedemann Paul<sup>3,4,7</sup> | Alexander Ulrich Brandt<sup>3,4,9</sup> | Jacqueline Palace<sup>1</sup>

<sup>1</sup>Nuffield Department of Clinical Neurosciences, University of Oxford, Oxford, UK

<sup>2</sup>Department of Neurology/Neuroimmunology, Multiple Sclerosis Centre of Catalonia (Cemcat), Hospital Universitari Vall d'Hebron, Universitat Autònoma de Barcelona, Barcelona, Spain

<sup>3</sup>Experimental and Clinical Research Center, Max Delbrück Center for Molecular Medicine and Charité – Universitätsmedizin Berlin, Corporate Member of Freie Universität Berlin, Humboldt-Universität zu Berlin, and Berlin Institute of Health, Berlin, Germany

<sup>4</sup>NeuroCure Clinical Research Center, Charité – Universitätsmedizin Berlin, Corporate Member of Freie Universität Berlin, Humboldt-Universität zu Berlin, and Berlin Institute of Health, Berlin, Germany

<sup>5</sup>Department of Pharmacology, University of Oxford, Oxford, UK

<sup>6</sup>Department of Neurology, National Neuroscience Institute, Singapore, Singapore

<sup>7</sup>Department of Neurology, Charité – Universitätsmedizin Berlin, Corporate member of Freie Universität Berlin, Humboldt-Universität zu Berlin, and Berlin Institute of Health, Berlin, Germany

<sup>8</sup>Berlin Institute of Health (BIH, Berlin, Germany)

<sup>9</sup>Department of Neurology, University of California Irvine, Irvine, CA, USA

## Correspondence

Alexander Ulrich Brandt, Translational Neuroimaging Group, Clinical Neuroimmunology, Experimental and Clinical Research Center, Charité – Universitätsmedizin Berlin, Laboradresse: Sauerbruchweg 5, Charitéplatz 1, 10117 Berlin, Germany.  
Emails: alexander.brandt@charite.de; aubrandt@uci.edu

## Funding information

Supported by the Einstein Foundation Berlin (Einstein Junior Scholarship to S.M.), the German Federal Ministry of

## Abstract

**Background and purpose:** Foveal changes were reported in aquaporin-4 antibody (AQP4-Ab) seropositive neuromyelitis optica spectrum disorder (NMOSD) patients; however, it is unclear whether they are independent of optic neuritis (ON), stem from sub-clinical ON or crossover from ON in fellow eyes. Fovea morphometry and a statistical classification approach were used to investigate if foveal changes in NMOSD are independent of ON and progressive.

**Methods:** This was a retrospective longitudinal study of 27 AQP4-IgG + NMOSD patients (49 eyes; 15 ON eyes and 34 eyes without a history of ON [NON eyes]), follow-up median (first and third quartile) 2.32 (1.33–3.28), and 38 healthy controls (HCs) (76 eyes),

**Abbreviations:** AQP4-Ab, aquaporin-4 antibody; ART, automatic real-time; FT, foveal thickness; GCIP, combined ganglion cell and inner plexiform layer volume; HC, healthy control; INL, inner nuclear layer; LME, linear mixed effects; NMOSD, neuromyelitis optica spectrum disorder; NON, eyes without history of optic neuritis; OCT, optical coherence tomography; ON, optic neuritis; OPLS-DA, orthogonal partial least squares discriminant analysis; pRNFL, peripapillary retinal nerve fibre layer; TMV, total macular volume; VIP, variable importance in projection.

Adriana Roca-Fernández and Frederike Cosima Oertel are equally contributing first authors.

Alexander Ulrich Brandt and Jacqueline Palace are equally contributing senior authors.

[Correction added on 21 April 2021, after first online publication: The author name Sedamirhosein Motamedi has been corrected to Seyedamirhosein Motamedi.]

This is an open access article under the terms of the Creative Commons Attribution-NonCommercial-NoDerivs License, which permits use and distribution in any medium, provided the original work is properly cited, the use is non-commercial and no modifications or adaptations are made.

© 2021 The Authors. *European Journal of Neurology* published by John Wiley & Sons Ltd on behalf of European Academy of Neurology.

Economic Affairs and Energy (BMW EXIST 03EFEBE079 to A.U.B.), German Research Foundation (DFG Exc. 257 to F.P. and A.U.B.), German Federal Ministry of Education and Research (BMBF Neu2 ADVISIMS to F.P. and A.U.B.) and Novartis (research grant to H.G.Z.) and Ministry of Health, Singapore, through the National Medical Research Council Research Training Fellowship (NMRC/Fellowship/0038/2016) (grant to T.Y.).

follow-up median (first and third quartile) 1.95 (1.83–2.54). The peripapillary retinal nerve fibre layer thickness and the volume of combined ganglion cell and inner plexiform layer as measures of neuroaxonal damage from ON were determined by optical coherence tomography. Nineteen foveal morphometry parameters were extracted from macular optical coherence tomography volume scans. Data were analysed using orthogonal partial least squares discriminant analysis and linear mixed effects models.

**Results:** At baseline, foveal shape was significantly altered in ON eyes and NON eyes compared to HCs. Discriminatory analysis showed 81% accuracy distinguishing ON vs. HCs and 68% accuracy in NON vs. HCs. NON eyes were distinguished from HCs by foveal shape parameters indicating widening. Orthogonal partial least squares discriminant analysis discriminated ON vs. NON with 76% accuracy. In a follow-up of 2.4 (20.85) years, no significant time-dependent foveal changes were found.

**Conclusion:** The parafoveal area is altered in AQP4-Ab seropositive NMOSD patients suggesting independent neuroaxonal damage from subclinical ON. Longer follow-ups are needed to confirm the stability of the parafoveal structure over time.

#### KEYWORDS

aquaporin-4 antibodies (AQP4-IgG), foveal morphometry, neuromyelitis optica spectrum disorders (NMOSD), optic neuritis, retinal neuroaxonal damage

## INTRODUCTION

Neuromyelitis optica spectrum disorders (NMOSDs) are relapsing inflammatory diseases of the central nervous system with a predilection for optic nerves, brainstem and spinal cord [1]. The discovery of pathogenic antibodies to astrocytic aquaporin-4 (AQP4) water channels [2] in the majority of patients [3,4] has led to NMOSD being categorized as a primary astrocytopathy, in which AQP4 antibodies (AQP4-Abs) cause complement-mediated damage to AQP4-expressing astrocytes [3].

Aquaporin-4 antibody seropositive NMOSD is defined by a relapsing course, but without chronic clinical progression or chronic lesion activity [5]. Acute optic neuritis (ON) is a frequent manifestation of AQP4-Ab seropositive NMOSD and is typically characterized by severe visual impairment [6], posterior involvement of the optic nerve on magnetic resonance imaging, severe damage neuropathologically [7] and neuroaxonal loss in the retina measured by optical coherence tomography (OCT) [8].

An increasing number of studies have reported retinal changes in NMOSD patient eyes with no known history of clinical ON [9–11]. This is supported by data from animal models of NMOSD, in which rats injected with AQP4-Abs show complement-independent Müller cell loss in the retina [12]. Müller cells are glial cells that extend longitudinally through the retina [13] and that express AQP4 in end feet covering retinal blood vessels [14,15]. Müller cell density is high in the parafoveal area, but it decreases in the central avascular foveal zone [16]. To specifically target this area in OCT a fovea morphometry on 3D macular OCT images was developed, which can reliably describe the foveal/parafoveal shape [17]. Using this approach, specific foveal changes in NMOSD were previously reported, which are distinct to

changes in multiple sclerosis patients, a disorder also leading to ON but without AQP4-Abs [18].

An alternative hypothesis is that foveal changes stem from ON attacks that do not reach clinical threshold or from chiasmal cross-over during an ON in the contralateral eye. Whilst the focus of this research has been on the fovea, previous studies also reported some degree of neuroaxonal damage in eyes without clinical ON [10]. When excluding patients with a history of ON, evidence for retinal neuroaxonal damage was still found [9] and neuronal loss in the ganglion cell layer may even be progressive [10] lending support to this hypothesis.

The aim of this study was to longitudinally describe parafoveal changes and their diagnostic potential in AQP4-Ab seropositive NMOSD.

## METHODS

### Study population

In this retrospective study of patients and controls followed in two longitudinal observational studies in Oxford and Berlin, NMOSD AQP4-Ab seropositive patients with no other ophthalmological or neurological disease and a minimum of 1 year clinical and OCT follow-up were included. Inclusion criteria were (1) a clinic diagnosis of AQP4-Ab seropositive NMOSD according to the 2015 diagnostic criteria [19]; (2) follow-up examinations with minimum longitudinal clinical and OCT imaging data of 1 year; (3) minimum age of 18 at baseline; (4) minimum of 1 year from ON to baseline; (5) macular OCT scan characteristics, 61 B-scans with 768 A-scans. Exclusion

criteria were ophthalmological or neurological comorbidities potentially influencing OCT results, insufficient OCT image quality, acute ON attacks in the last 12 months or ON attacks during follow-up. Data from healthy age and sex matched controls were selected from both centres' image databases; longitudinal OCT data for healthy controls (HCs) was only available from the Berlin site. A flow diagram of the study cohort is presented in Figure 1.

## Optical coherence tomography

All participants were scanned on Spectralis spectral domain devices (Heidelberg Engineering, Heidelberg, Germany) with automatic real-time (ART) function for image averaging. The peripapillary retinal nerve fibre layer (pRNFL) was measured with an activated eye tracker using 3.4-mm ring scans around the optic nerve (Berlin and Oxford: 12°, 1536 A-scans, 1 ≤ ART ≤ 99). Combined ganglion cell layer and inner plexiform layer volume (GCIP), total macular volume (TMV), inner nuclear layer (INL) and retinal nerve fibre layer at the macula were calculated as a 3-mm diameter cylinder around the fovea for a macular volume scan (Berlin, 25° × 30°, 61 vertical B-scans, 11 ≤ ART ≤ 18; Oxford, 30° × 25°, 61 vertical B-scans, 17 ≤ ART ≤ 22). Foveal thickness (FT) was measured as the mean thickness of a 1-mm diameter cylinder around the fovea for the macular scan between the internal limiting membrane and the Bruch's membrane. Intraretinal semi-automatic segmentation was performed by the same experienced rater (FCO) for all data with HEYEX software (version 1.10.4.0 with viewing module 1.0.16.0., Heidelberg Engineering) to correct segmentation errors and discard scans of insufficient quality. OCT data presented in this study follow OSCAR-IB quality criteria [20] and APOSTEL recommendations [21]

## Fovea morphometry

To characterize the foveal shape, a 3D modelling algorithm was applied to macular OCT scans, applying parametric modelling of the

fovea using cubic Bèzier equations for foveal morphometry [17]. The method extracts foveal measurements such as depth, diameter, slope, pit and areas and volumes of different regions (Figure 2a). A detailed parameter overview is provided in Appendix A.

## Statistical methods

Group differences between AQP4-Ab seropositive NMOSD patients and HCs were tested by Fisher's exact tests for sex and by the Mann-Whitney *U* test for age. Multivariate analysis was used to analyse baseline and longitudinal differences for OCT and foveal shape parameters. Linear mixed effects (LME) models were applied to account for inter-eye correlations of monocular measurements. The initial model used for all the parameters was 'OCT ~ Age at baseline + Sex + Site + Group, random = ~1|Eye' for baseline and a nested LME model described as 'OCT ~ Age at baseline + Sex + Site + Group × time since baseline, random = ~1|Patient/Eye' for the longitudinal analysis. From the initial models, simpler models were built by discarding not significant fixed effects, to avoid overfitting the model.

Group comparisons were established both at baseline and longitudinally by obtaining estimated marginal means for the mixed effects model and contrasts of estimated marginal means were computed of all pairwise comparisons of least squares means.

After this, orthogonal partial least squares discriminant analysis (OPLS-DA) was applied to identify the best combination of foveal and macular measure to discriminate the NMOSD AQP4-Ab seropositive patients from HCs. OPLS-DA is a supervised multivariate analysis approach used to investigate the variables that are responsible for class discrimination between disease groups [22]. Nineteen foveal and six macular parameters from each patient were included in the model. In brief, after correction for unequal class sizes, 10-fold external cross-validation was performed; this entails splitting the foveal and macular data into a training set (using 90% of data) and a test set (using 10% of data) a total of 10 times to ensure that each sample appears in the test set exactly once. The test set is applied

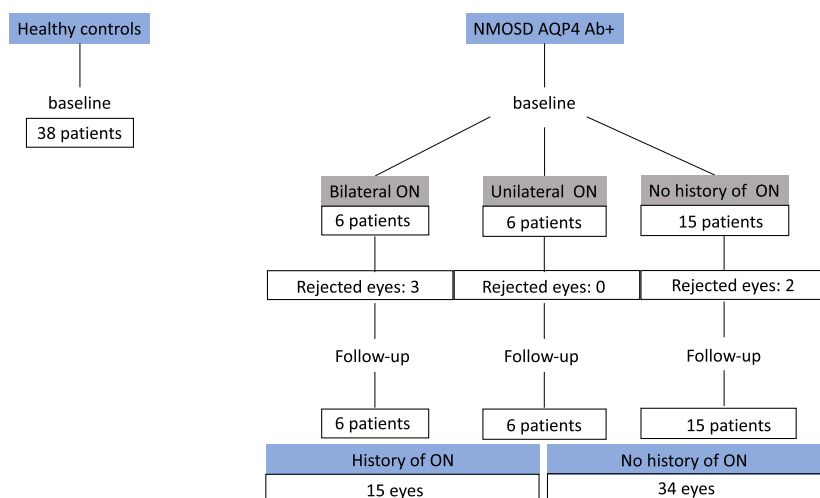


**FIGURE 1** Study cohort and follow-up flowchart. Flowchart of participants in the cohort study. NMOSD, neuromyelitis optica spectrum disorders; AQP4-ab+, aquaporin-4 antibody positive; ON, optic neuritis eyes [Colour figure can be viewed at [wileyonlinelibrary.com](https://onlinelibrary.wiley.com/terms-and-conditions)]

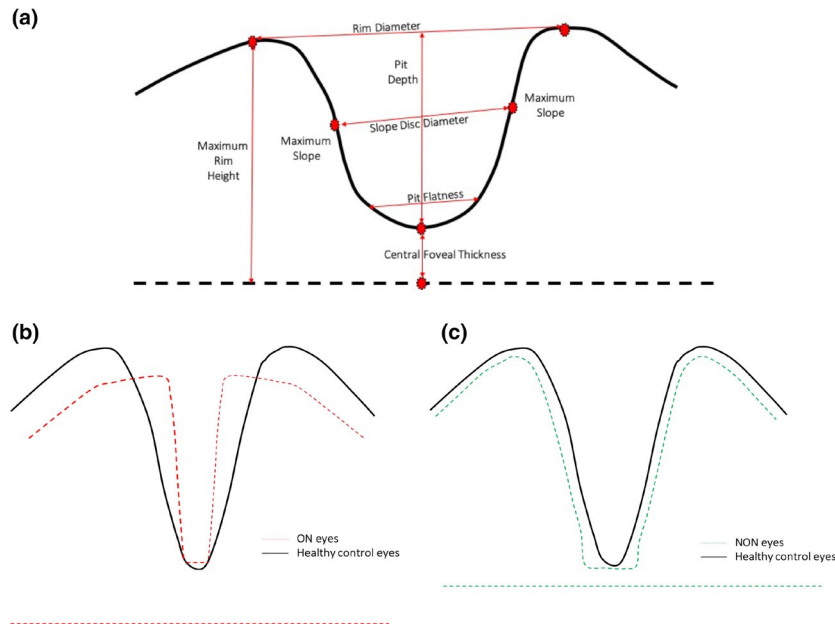


**FIGURE 2** Foveal changes in NMOSD. (a) Cross-sectional, 2D illustration on a central B-scan of foveal region parameters extracted with the CuBe algorithm [17]. (b) Eyes with a history of ON (ON eyes) and (c) eyes without a history of ON (NON eyes). Both horizontal dashed lines in (b) and (c) refer to the central foveal thickness distance, defined as the minimum height of the fovea at the centre of the pit. ON, optic neuritis; NON, non-optic neuritis [Colour figure can be viewed at [wileyonlinelibrary.com](http://wileyonlinelibrary.com)]

to the OPLS-DA model (generated using only the training set) to determine the predictive accuracy on independent (previously unseen) data. This process was repeated 100 times to produce 1000 models in total. If these models perform better than models produced by random class assignments (50%) then separation of the two groups has not occurred by chance and the model is statistically significant [23,24]. To identify the most important foveal/macular parameters responsible for the separation between patient groups, variable importance in projection (VIP) scores were generated. A VIP score is a measure of a parameter's importance to the OPLS-DA model: the higher the VIP score, the more importantly the parameter contributes towards the separation of patient groups. OPLS-DA was performed using in-house scripts and the `ropls` package in R software [23,25].

Statistical significance was established at  $p < 0.05$ . All tests and graphical representations were performed in R 3.6.2 with packages `nlme`, `ropls`, `ggplot2` and `emmeans`.

## RESULTS

### Cohort overview

Thirty-eight HCs and 27 AQP4-Ab seropositive NMOSD patients were included in the analysis (Table 1). Of the AQP4-Ab seropositive NMOSD group, 34 eyes never had a history of ON (NON), and 15 had a history of ON. Four eyes were excluded from the analysis due to poor image quality or technical issues, one eye due to amblyopia.

There were no significant differences between the HCs and the NMOSD group in the baseline demographic.

Group differences at baseline analysed using multivariate LME models with estimated marginal means adjusted for age at baseline, sex and site whilst accounting for inter-eye correlations are presented in detail in Table 2. As expected, the models showed significant thinning in pRNFL, GCIP, TMV and retinal nerve fibre layer at the macula in ON eyes compared to HC eyes, suggesting profound neuroaxonal damage. NON vs. HC eyes showed significantly thinner GCIP, TMV, INL and FT, but changes were less severe than in the ON eyes (Table 2).

### Foveal changes

Fovea morphometry quantifies several metrics of the fovea (Figure 2a). Visually, ON-related changes in the fovea/parafoveal area appear as flattened, whereas NON changes appear to be widened, already suggesting different mechanisms causing the change (Figure 2b,c). Lower values for ON vs. HC eyes were found in the following parameters: average pit depth, average rim height, average rim diameter, rim disc area, major and minor rim disc length, pit volume and average maximum pit slope degree. ON vs. NON eyes showed significantly lower values for average pit depth, average rim height, average rim diameter, minor slope disc length, slope disc area, rim disc area, major and minor rim disc length, pit volume and average maximum pit slope degree. NON vs. HC eyes showed significantly lower values for average rim height and higher values for minor slope disc length, slope disc area, average slope disc diameter,

pit disc area, average pit flat disc diameter, and major and minor pit flat disc length (Table 2 and Appendix A, Figure A2).

## Discriminatory analysis

Orthogonal partial least squares discriminant analysis identifies a linear combination of measures to separate two groups, with the aim of being able to classify individual patients. This method reduces the weight of tightly correlated values that do not give additional benefit. OPLS-DA was employed as a supervised statistical method to discriminate ON from HCs, ON vs. NON and NON eyes from HCs. The mean predictive accuracy of the OPLS-DA models distinguishing ON vs. HC eyes was  $81.16\% \pm 5.39\%$  ( $p < 0.0001$ ), whilst the mean predictive accuracies of the OPLS-DA models separating ON vs. NON eyes and ON eyes vs. HCs were  $76.48\% \pm 5.33\%$  ( $p < 0.0001$ ) and  $67.71\% \pm 4.77\%$  ( $p < 0.0001$ ) respectively (Figure 3).

Importantly, the top nine most discriminatory variables contributing to the separation of ON eyes from HC and NON eyes are pRNFL, GCIP, rim volume, major and minor rim disc length, average rim diameter, rim disc area, average pit depth and average rim height. In the case of the separation between NON eyes and HCs, the top nine most discriminatory variables were TMV, average rim height, GCIP, average pit flat disc diameter, major and minor pit flat disc length, pit disc area, INL and FT (Figure 3). The selection of largely different morphometrical factors in ON and NON eyes clearly suggest that, whilst NON eyes show some evidence of neuroaxonal damage, this damage cannot explain the foveal shape changes. The variables that better describe the difference between HC and NON eyes are not at the retinal or peripapillary level but at foveal level, indicating an unlikely effect of a subclinical ON and/or a chiasmal crossover effect from a contralateral ON, but being more in line with a primary astrocytopathy effect.

**TABLE 1** Cohort overview

	HCs	NMOSD	
		ON	NON
Number of participants	38	12 <sup>a</sup>	21 <sup>a</sup>
Number of eyes	76	15 <sup>b</sup>	34 <sup>b</sup>
Sex			
Female <i>n</i> (%)	27 (74%)	10 (83%)	20 (95%)
Age at baseline (years)			
Median (1st–3rd quartile)	42.60 (30.65–51.77)	38.75 (25.65–49.17)	46.00 (38.60–52.40)
F/U time (years)			
Median (1st–3rd quartile)	1.95 (1.83–2.54)	2.765 (1.022–3.280)	2.44 (1.76–3.28)
Race			
African/Caribbean <i>n</i> (%)	Not available	2 (17%)	3 (14%)
Asian <i>n</i> (%)		1 (8%)	2 (10%)
Caucasian <i>n</i> (%)		8 (67%)	16 (76%)
Mix <i>n</i> (%)		1 (8%)	
Disease duration (years)			
Median (1st–3rd quartile)	Not applicable	1.16 (0.39–3.70)	1.90 (0.54–5.80) <sup>c</sup>
Time from last ON (years)			
Median (1st–3rd quartile)		4.21 (1.94–9.27)	3.66 (2.15–8.35) <sup>c</sup>

Note: Age and sex group differences between HCs and NMOSD patients were not significant (Fisher's exact tests for sex, estimate 4.37,  $p = 0.1020$ ; Mann–Whitney test for age, estimate 3.19,  $p = 0.3796$ ; follow-up time, estimate  $-0.33$ ,  $p = 0.17$ ).

Abbreviations: F/U, follow-up; HCs, healthy controls; NMOSD, neuromyelitis optica spectrum disorder; NON, non-optic neuritis; ON, optic neuritis.

<sup>a</sup>Six patients with bilateral ON, six patients with unilateral ON and 15 patients with no history of ON. ON = 6 + 6 and NON = 6 + 15.

<sup>b</sup>Eyes counted after the exclusion of five eyes.

<sup>c</sup>Based on unilateral ON eyes.

TABLE 2 Baseline OCT measurements

	NMOSD				LME					
	HCs		NON		ON vs. HCs		NON vs. HCs		ON vs. NON	
	Mean (SD)	Mean (SD)	Mean (SD)	Mean (SD)	B (SE)	p value	B (SE)	p value	B (SE)	p value
pRNFL (µm)	99.10 ± 10.35	61.86 ± 21.72	98.17 ± 10.86	98.17 ± 10.86	-37.23 (3.48)	<0.0001	-0.929 (2.54)	1	-36.310 (3.82)	<0.0001
GCIP (mm <sup>3</sup> )	0.62 ± 0.04	0.40 ± 0.11	0.57 ± 0.05	0.57 ± 0.05	-0.2099 (0.0170)	<0.0001	-0.0539 (0.0124)	0.0001	-0.1561 (0.0189)	<0.0001
TMV (mm <sup>3</sup> )	2.36 ± 0.09	2.1 ± 0.13	2.28 ± 0.07	2.28 ± 0.07	-0.1901 (0.0262)	<0.0001	-0.0863 (0.0192)	<0.0001	-0.1038 (0.0291)	0.0016
INL (mm <sup>2</sup> )	0.27 ± 0.02	0.28 ± 0.02	0.25 ± 0.02	0.25 ± 0.02	0.009 (0.006)	0.4456	-0.01 (0.004)	0.0072	0.02 (0.007)	0.0028
FT (µm)	275.10 ± 19.58	268.13 ± 19.39	264 ± 18.61	264 ± 18.61	-5.56 (5.39)	0.9121	-12.46 (3.96)	0.0062	6.90 (6)	0.7570
mRNFL (mm <sup>3</sup> )	0.14 ± 0.01	0.12 ± 0.03	0.14 ± 0.01	0.14 ± 0.01	-0.01874 (0.00440)	0.0001	-0.00267 (0.00323)	1	-0.01606 (0.00490)	0.0041
Average pit depth (mm)	0.11 ± 0.02	0.08 ± 0.01	0.11 ± 0.02	0.11 ± 0.02	-0.0371 (0.00622)	<0.0001	-0.0062 (0.0045)	0.5230	-0.0309 (0.00682)	<0.0001
Central foveal thickness (mm)	0.23 ± 0.01	0.23 ± 0.01	0.22 ± 0.01	0.22 ± 0.01	0.001 (0.005)	1	-0.004 (0.003)	0.407	0.007 (0.005)	0.656
Average rim height (mm)	0.34 ± 0.01	0.31 ± 0.02	0.33 ± 0.01	0.33 ± 0.01	-0.0344 (0.0398)	<0.0001	-0.0133 (0.00292)	<0.0001	-0.0211 (0.00443)	<0.0001
Average rim diameter (mm)	2.19 ± 0.12	2.02 ± 0.05	2.17 ± 0.13	2.17 ± 0.13	-0.1649 (0.0344)	<0.0001	-0.0232 (0.0244)	1	-0.1417 (0.0376)	0.0008
Rim disc area (mm <sup>2</sup> )	3.75 ± 0.40	3.20 ± 0.17	3.67 ± 0.44	3.67 ± 0.44	-0.5507 (0.1162)	<0.0001	-0.0765 (0.0824)	1	-0.4742 (0.1268)	0.0009
Major rim disc length (mm)	0.63 ± 0.069	0.54 ± 0.03	0.62 ± 0.07	0.62 ± 0.07	-0.0953 (0.0198)	<0.0001	-0.0136 (0.0140)	0.9988	-0.0817 (0.0216)	0.0007
Minor rim disc length (mm)	0.62 ± 0.068	0.53 ± 0.02	0.61 ± 0.07	0.61 ± 0.07	-0.0896 (0.0194)	<0.0001	-0.0121 (0.0137)	1	-0.0775 (0.021)	0.0011
Major slope disc length (mm)	0.07 ± 0.02	0.06 ± 0.021	0.08 ± 0.03	0.08 ± 0.03	-0.007 (0.008)	1.000	0.013 (0.006)	0.1003	-0.021 (0.009)	0.075
Minor slope disc length (mm)	0.05 ± 0.02	0.05 ± 0.02	0.07 ± 0.02	0.07 ± 0.02	-0.00496 (0.00668)	1	0.01625 (0.00490)	0.0036	-0.2121 (0.00743)	0.0152
Slope disc area (mm <sup>2</sup> )	0.40 ± 0.15	0.366 ± 0.12	0.48 ± 0.18	0.48 ± 0.18	-0.0338 (0.448)	1	0.0854 (0.0327)	0.0304	-0.1192 (0.0491)	0.0502
Average slope disc diameter (mm)	0.69 ± 0.14	0.66 ± 0.12	0.76 ± 0.15	0.76 ± 0.15	-0.274 (0.0407)	1	0.0719 (0.0297)	0.0514	-0.0993 (0.0447)	0.0842
Pit disc area (mm <sup>2</sup> )	0.03 ± 0.01	0.044 ± 0.015	0.04 ± 0.01	0.04 ± 0.01	0.00639 (0.00371)	0.261	0.00936 (0.00271)	0.0023	-0.00296 (0.00407)	1
Average pit flat disc diameter (mm)	0.21 ± 0.03	0.23 ± 0.04	0.24 ± 0.03	0.24 ± 0.03	0.01721 (0.01039)	0.3006	0.02597 (0.00759)	0.0025	-0.00876 (0.01140)	1
Major pit flat disc length (mm)	0.006 ± 0.002	0.008 ± 0.002	0.008 ± 0.002	0.008 ± 0.002	0.00121 (0.000669)	0.2216	0.00158 (0.000488)	0.0048	-0.00037 (0.000734)	1
Minor pit flat disc length (mm)	0.005 ± 0.001	0.0068 ± 0.002	0.007 ± 0.002	0.007 ± 0.002	0.000937 (0.000586)	0.3378	0.001540 (0.000428)	0.0014	-0.000603 (0.000643)	0.3378

(Continues)



TABLE 2 (Continued)

	HCs		NMOSD		LME							
	Mean (SD)		ON		NON		ON vs. HCs		NON vs. HCs		ON vs. NON	
	Mean (SD)		Mean (SD)		Mean (SD)		B (SE)	p value	B (SE)	p value	B (SE)	p value
Rim volume (mm <sup>3</sup> )	1.04 ± 0.15		0.79 ± 0.10		0.97 ± 0.15		-0.25 (0.043)	<0.0001	-0.07(0.031)	0.0662	-0.183(0.043)	0.0006
Pit volume (mm <sup>3</sup> )	0.26 ± 0.04		0.21 ± 0.032		0.26 ± 0.04		-0.05250 (0.01307)	0.0003	0.00148 (0.00955)	1	0.05398 (0.01434)	0.0008
Inner rim volume (mm <sup>3</sup> )	0.10 ± 0.01		0.09 ± 0.01		0.09 ± 0.01		0.00409 (0.00539)	1	-0.00967 (0.00394)	0.0464	0.00559 (0.00592)	1
Average maximum pit slope degree (°)	11.67 ± 3.38		7.87 ± 2.57		11.02 ± 2.88		-3.798 (0.896)	0.0001	-0.652 (0.654)	0.9639	-3.146 (0.983)	0.0053

Notes: Baseline OCT and foveal results and baseline comparisons for patients with NMOSD (ON and NON) and HCs. Maximum likelihood was used for the estimation of *p* values.

Abbreviations: B, estimate; FT, foveal thickness; GCIP, combined ganglion cell and inner plexiform layer volume; HCs, healthy controls; INL, inner nuclear layer; LME, linear mixed effects; mRNFL, retinal nerve fibre layer at the macula; NMOSD, neuromyelitis optica spectrum disorder; NON, eyes without a history of optic neuritis; OCT, optical coherence tomography; ON, eyes with a history of optic neuritis; pRNFL, peripapillary retinal nerve fibre layer at the disc; SE, standard error; TMV, total macular volume.

Bold values indicate significant result (*p* ≤ 0.05).

## Longitudinal changes

After OPLS-DA indicated that foveal shape changes in NON eyes are unlikely to be attributable to neuroaxonal damage to the optic nerve, potential longitudinal changes were then investigated. The analysis was limited on NON eyes to not overlay ON-unrelated changes with potential changes from ON. Annualized changes from baseline to last follow-up for the NON eyes are summarized in Table 3. In summary, longitudinal analysis using LME models identified no significant changes in any of the foveal parameters at follow-up compared to baseline (Table 3). Standard ring scan and macular parameters also did not change significantly in comparison to HCs (not shown).

## DISCUSSION

Our study provides evidence that the parafoveal area, which is rich in AQP4-expressing Müller cells, is altered in AQP4-Ab seropositive NMOSD patients who never experienced clinical ON, and suggests that these changes are likely to be independent of neuroaxonal damage from subclinical ON, as macular and peripapillary layers were not affected in this subset. No evidence was found that these foveal changes are progressive in a longitudinal follow-up.

## Neuroaxonal damage and foveal/parafoveal changes from optic neuritis

Optic neuritis causes neuroaxonal damage in NMOSD, and this damage is reflected by pRNFL thickness loss reflecting axonal damage and GCIP loss reflecting neuronal ganglion cell loss [9,10,26,27]. ON in NMOSD typically affects posterior segments of the optic nerve, often with involvement of the optic chiasm [28]. Consequently, in some cases, inflammatory activity due to chiasmal crossover fibres from an ON eye may have partial involvement of the contralateral side, which may be overlooked in clinical assessment [29]. Our study shows that ON also leads to foveal changes, which can best be described as flattening of the parafoveal ring: OPLS-DA selected primarily parameters of neuroaxonal damage (pRNFL, GCIP) as well as parameters describing the volume and flatness of the fovea, namely a decrease in rim volume, major rim disc length, average rim diameter, rim disc area and others.

## Are foveal changes independent of optic neuropathy?

Eyes without a history of ON also showed significant GCIP but not pRNFL loss in our study, which is in line with previous studies showing ON-independent retinal changes in NMOSD [9,11]. This could be explained by the fact that GCIP measurements were performed in the parafoveal area, whilst pRNFL reflects the neuroaxonal content of the whole eye. Hence, pRNFL measures may not be as proportionally damaged as GCIP measured regionally. GCIP loss was much less

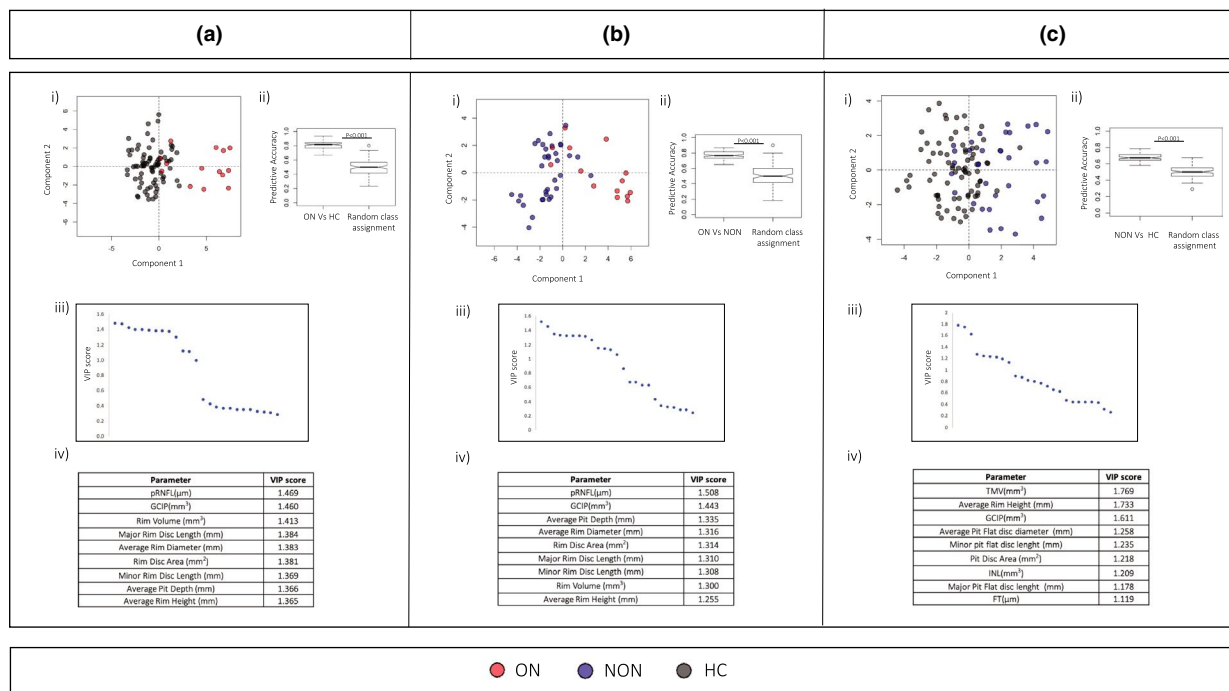


**FIGURE 3** OPLS-DA results. (ai) OPLS-DA, ON vs. HC eyes comparison (accuracy 81.16%); (aii) OPLS-DA, ON vs. HC eyes model validation; (aiii) VIP scores from all parameters used in the model for each comparison; (aiv) values of the most important parameters for ON vs. HC eyes. (bi) OPLS-DA, ON vs. NON eyes comparison (accuracy 76.48%); (bii) OPLS-DA, ON vs. NON eyes model validation; (biii) VIP scores from all parameters used in the model for each comparison; (biv) values of the most important parameters for ON vs. NON eyes. (ci) OPLS-DA, NON vs. HC eyes comparison (accuracy 67.71%); (cii) OPLS-DA, NON vs. HC eyes model validation; (ciii) VIP scores from all parameters used in the model for each comparison; (civ) values of the most important parameters for NON vs. HC eyes. OPLS-DA, orthogonal partial least squares discriminatory analysis; VIP, variable importance in projection; ON, optic neuritis; NON, non-optic neuritis; HC, healthy control; pRNFL, peripapillary retinal nerve fibre layer; GCIP, ganglion cell and inner plexiform layer volume; INL, inner nuclear layer; FT, foveal thickness [Colour figure can be viewed at [wileyonlinelibrary.com](https://onlinelibrary.com)]

pronounced than in ON eyes. In a previous study potential progressive GCIP loss in NMOSD patients was reported regardless of ON [10]. Previously, FT changes on OCT in NMOSD AQP4-Ab seropositive patients were also reported [9,11]. Fovea morphometry changes were also identified not only comparing against HCs but also when compared to multiple sclerosis patients [18]. Here it is shown that, in contrast to ON eyes, the fovea of NON eyes was characterized by wider pits and more pronounced slopes, best described as foveal widening. OPLS-DA selected parameters TMV, average rim height, average pit flat disc diameter, minor pit flat disc length, pit disc area and others as best discriminatory against HCs. Importantly, OPLS-DA selected parameters differed significantly between ON and NON eyes, lending strong support to the hypothesis that the observed foveal changes in NON eyes are not caused by neuroaxonal damage to the optic nerve.

Ours and previous clinical studies did not address the underlying aetiology of foveal involvement in AQP4-Ab seropositive NMOSD. The parafoveal area is rich in Müller cells, the principal astrocytic glia of the retina, which express AQP4 in their end feet adjacent to retinal vessels [30]. In an animal model of retinal damage in NMOSD, AQP4-Ab injection into the vitreous resulted in reactive changes and loss of Müller cells without complement activation [12]. Previous studies have demonstrated lack of

complement reactivity in the area postrema [31] this could also be the case in the retina, where AQP4-Ab would still bind the retinal AQP4-expressing cells but would fail to activate the complement, and therefore would not cause mediated damage in the retinal cell integrity but still would make the changes in the foveal morphometry.

## Longitudinal observations

In a previous study progressive GCIP loss in AQP4-Ab seropositive NMOSD regardless of ON was reported [10]. In contrast, in the current study no evidence for overt progressiveness of foveal shape changes in NON eyes was found. Given the sample size limitation of this study, it is unclear whether it was simply underpowered or whether changes to the fovea are indeed not progressive. Interestingly, OPLS-DA selected GCIP but not pRNFL as one of the strongest parameters discriminating NON eyes from HCs. It is possible that GCIP changes reflect a neurodegenerative reaction of ganglion cells to Müller cell affection. It is possible that GCIP changes reflect a neurodegenerative reaction of ganglion cells to Müller cell affection. The discrepancy between pRNFL and GCIP differences in NON eyes is interesting and warrants further investigation. Future studies with greater sample size and higher power



**TABLE 3** Annualized foveal changes

	NMOSD-NON	NMOSD-NON F/U vs baseline	<i>p</i> value
	Annualized change, mean (SD)	<i>B</i> (SE)	
<b>Macular parameters</b>			
pRNFL (μm)	-0.611 ± 1.85	-0.11563 (0.276813)	0.6767
GCIPL (mm <sup>3</sup> )	-0.009 ± 0.0044	-0.0007202 (0.000816)	0.3788
TMV (mm <sup>3</sup> )	-0.004 ± 0.013	-0.0028363 (0.002249)	0.2090
INL (mm <sup>3</sup> )	0.003 ± 0.001	-0.00044411 (0.000955)	0.6427
FT (μm)	-0.43 ± 2.19	-0.61538 (0.429695)	0.1538
RNFL (mm <sup>3</sup> )	-0.0003 ± 0.006	-0.00122806 (0.000881)	0.1653
<b>Foveal parameters</b>			
Average pit depth (mm)	0.00012 ± 0.002	0.0004 (0.0004)	0.3149
Central foveal thickness (mm)	-0.0005 ± 0.0001	-0.0004 (0.0004)	0.3891
Average rim height (mm)	-0.00038 ± 0.0023	-0.0000040 (0.00039)	0.9918
Average rim diameter (mm)	-0.00088 ± 0.01	-0.00059 (0.002)	0.8039
Rim disc area (mm <sup>2</sup> )	-0.0029 ± 0.04	-0.001 (0.007)	0.8040
Major rim disc length (mm)	2.38 E-05 ± 0.009	0.0000439 (0.0013)	0.9746
Minor rim disc length (mm)	-0.0009 ± 0.007	-0.00067 (0.0016)	0.6194
Major slope disc length (mm)	-0.001 ± 0.005	-0.001 (0.0008)	0.157
Minor slope disc length (mm)	-0.001 ± 0.004	-0.00017 (0.0006)	0.803
Slope disc area (mm <sup>2</sup> )	-0.01 ± 0.026	-0.004 (0.004)	0.35
Average slope disc diameter (mm)	-0.006 ± 0.02	-0.002 (0.003)	0.49
Pit disc area (mm <sup>2</sup> )	-0.0002 ± 0.002	-0.0002 (0.0006)	0.6445
Average pit flat disc diameter (mm)	-0.0008537 ± 0.006	-0.001 (0.00146)	0.4528
Major pit flat disc length (mm)	-7.97E-05 ± 0.0004	-0.00008 (0.00011)	0.4782
Minor pit flat disc length (mm)	1.25 E-05 ± 0.0005	-0.000016 (0.00008)	0.8469
Rim volume (mm <sup>3</sup> )	0.000333 ± 0.017	0.00010 (0.0030)	0.9721
Pit volume (mm <sup>3</sup> )	-0.0020 ± 0.008	-0.0003 (0.001)	0.77
Inner rim volume (mm <sup>3</sup> )	0.00022 ± 0.002	-0.00002 (0.0004)	0.96
Average maximum pit slope degree (°)	0.0034 ± 0.41	-0.041 (0.079)	0.599

Note: Significant *p* values are shown in bold. Maximum likelihood was used for the estimation of *p* values.

Abbreviations: *B*, estimate; FT, foveal thickness; F/U, follow-up; GCIPL, combined ganglion cell and inner plexiform layer volume; INL, inner nuclear layer; NMOSD-NON, neuromyelitis optica spectrum disease eyes with no history of optic neuritis; pRNFL, peripapillary retinal nerve fibre layer; SE, standard error; TMV, total macular volume.

are required to address this. The annual changes reported in this study, albeit not significant, may serve as a basis for sample size calculations.

## Functional relevance

The fovea is the most important region for functional vision in the retina [32]. Due to the high concentration of cones, the fovea is responsible for central vision and involved in high-resolution image formation [33]. ON in NMOSD is associated with often severe visual function loss [6]. A recent study found that patients with AQP4-Ab seropositive NMOSD had worse visual outcomes compared to multiple sclerosis patients and patients with myelin oligodendrocyte glycoprotein antibody seropositive disease in relation to their actual ganglion cell loss [34]. Further studies are warranted to confirm the

clinical relevance and to identify potential avenues for symptomatic treatment.

## Relevance for other central nervous system areas

Whilst our findings are limited to the retina, the observation that there may be subtle AQP4-related damage in NMOSD is also relevant for other central nervous system areas. Secondary symptoms in NMOSD like cognitive dysfunction [35] fatigue [36] pain [37] and mood disorders [38] are yet mostly unexplained. Imaging studies have so far been inconclusive regarding focal damage to brain structures in NMOSD, Imaging studies have so far been inconclusive regarding focal damage to brain structures in NMOSD happening outside of attack-related areas or potentially caused by a secondary axonal or transsynaptic

neurodegeneration [39–41]. A recent independent study has identified the nucleus accumbens as a potentially interesting target with functional relevance of AQP4-expressing cells for neural plasticity [42].

## Limitations and strengths

An important limitation of our study is the small number of NON eyes, which prevents us from separately analysing patients with contralateral ON and those never having ON. Additionally, most patients presenting with an acute long extensive transverse myelitis and no visual symptoms will not have extensive visual and OCT testing to investigate subtle ON. A recent publication [43] investigating latency delay and amplitude reduction in visual evoked potentials in patients with no history of ON suggests that attack-unrelated sub-clinical disease activity may be happening in the visual system; one of the limitations of this study is the lack of visual evoked potential data that could shed light on how this process happens.

A major strength of this paper is the use of a novel parametric modelling of the 3D foveal shape using cubic Bèzier equations [17]. This has allowed us to describe the fovea and parafoveal area in an objective and reproducible way. Our cohort, constituted only of AQP4-Ab seropositive patients, sets the first step on clinical significance ensuring the examination of only one disease process. Further, our results suggest that foveal morphometry may offer clinical diagnostic utility. However, broad application would require further validation across alternative platforms and protocols.

## CONCLUSION

In summary, evidence is provided that the fovea is wider in NON eyes in patients with NMOSD, whereas ON eyes typically present with a flatter fovea compared to HCs and NON eyes. Discriminatory analysis strongly suggests that changes in NON eyes are not caused by subclinical optic neuropathy or ON. Our study supports a model in which AQP4-Abs affect antigen-expressing glial cells in NMOSD, in this case Müller cells, without complement involvement. This has relevance for the pathological understanding of NMOSD as well as potential clinical implications.

## ACKNOWLEDGEMENTS

To Dr Sunil Yadav for foveal morphometry model definitions. Open Access funding enabled and organized by Projekt DEAL. WOA Institution: Charite Universitätsmedizin Berlin Blended DEAL: Projekt DEAL

## CONFLICT OF INTEREST

A Roca-Fernandez has no competing interests. FC Oertel was employed by Nocturne, unrelated to this project. T Yeo has received travel grants from UCB, Merck and PACTRIMS, and travel awards from ACTRIMS and Orebro University. S Motamedi is named as co-inventor on the patent application for the fovea

morphometry method used in this paper ('Method for estimating shape parameters of the fovea by optical coherence tomography', International Publication Number WO 2019/016319 A1), related to this work. F Probert has no competing interests. MJ Craner has received honoraria for educational events and/or consultancy from Biogen, Merck, Roche, AbbVie and Novartis. J Sastre-Garriga declares grants and personal fees from Genzyme, personal fees from Almirall, Biogen, Celgene, Merck, Bayer, Biopass, Bial, Novartis, Roche and Teva, outside the submitted work; he is Associate Editor of *Multiple Sclerosis Journal* and Scientific Director of Revista de Neurologia, outside the submitted work. HG Zimmermann received research grants from Novartis and speaking honoraria from Bayer Healthcare. S Asseyer received travel grants from Celgene GmbH, unrelated to this project. J Kuchling received congress registration fees from Biogen, speaker honoraria from Sanofi Genzyme and Bayer Schering, and research support from Krankheitsbezogenes Kompetenznetz, Multiple Sklerose (KKNMS), not related to this work. JK is a participant in the BIH-Charité Junior Clinician Scientist Program funded by the Charité – Universitätsmedizin Berlin and Berlin Institute of Health. J Bellmann-Strobl has received travel grants and speaking honoraria from Bayer Healthcare, Biogen Idec, Merck Serono, Sanofi Genzyme, Teva Pharmaceuticals, Roche and Novartis, none of them related to preparing this paper. K Ruprecht was supported by the German Ministry of Education and Research (BMBF/KKNMS, Competence Network Multiple Sclerosis) and has received research support from Novartis and Merck Serono as well as speaking fees and travel grants from Guthy Jackson Charitable Foundation, Bayer Healthcare, Biogen Idec, Merck Serono, sanofi-aventis/Genzyme, Teva Pharmaceuticals, Roche and Novartis. MI Leite reports funding from NHS National Specialised Commissioning Group for Neuromyelitis Optica, UK, and the NIHR Oxford Biomedical Research Centre, UK; and speaker honoraria or travel grants from Biogen Idec, Novartis and the Guthy-Jackson Charitable Foundation. F Paul is named as co-inventor on the patent application for the fovea morphometry method used in this paper ('Method for estimating shape parameters of the fovea by optical coherence tomography', International Publication Number WO 2019/016319 A1), related to this work; Dr Paul is cofounder and holds shares in technology start-up Nocturne GmbH, which has commercial interest in OCT applications in neurology and declares that he has received research grants and speaker's honoraria from Bayer Healthcare, Teva Pharmaceuticals, Genzyme, Merck and Co., Novartis and MedImmune. He is also a member of the steering committee for the OCTIMS study (run by Novartis). AU Brandt is named as co-inventor on the patent application for the fovea morphometry method used in this paper ('Method for estimating shape parameters of the fovea by optical coherence tomography', International Publication Number WO 2019/016319 A1), related to this work. Dr Brandt is cofounder and shareholder of technology start-ups Motognosis and Nocturne. He is named as inventor on several patent applications describing multiple sclerosis serum biomarkers, perceptive visual computing for motor function assessment and retinal image analysis. J Palace reported receiving grants from the National Health Service to

conduct a national congenital myasthenia service and neuromyelitis service, the Multiple Sclerosis Society, Guthrie Jackson Foundation, Chugai, and MedImmune; personal fees from Teva, Novartis, Roche, MedDay and ARGEX; and grants and personal fees from Merck Serono, Biogen, Alexion, and ABIDE, Genzyme and MedImmun. No other disclosures were reported.

## AUTHOR CONTRIBUTIONS

Adriana Roca-Fernandez: Conceptualization (equal); data curation (lead); formal analysis (lead); funding acquisition (equal); investigation (lead); methodology (lead); visualization (equal); writing original draft (lead). Frederike Cosima Oertel: Conceptualization (equal); data curation (equal); investigation (equal); methodology (equal); supervision (equal); writing original draft (equal); writing review and editing (equal). Tianrong Yeo: Formal analysis (equal); supervision (supporting); writing review and editing (equal). Seyedamirhosein Motamedi: Data curation (supporting); formal analysis (equal); investigation (equal); methodology (equal); software (equal); visualization (equal); writing review and editing (equal). Fay Probert: Methodology (equal); software (equal); visualization (equal); writing review and editing (equal). Matthew Craner: Conceptualization (equal); investigation (equal); methodology (equal); resources (equal); supervision (equal); writing review and editing (equal). Jaume Sastre-Garriga: Investigation (equal); resources (equal); writing review and editing (equal). Hanna Zimmermann: Conceptualization (equal); data curation (equal); investigation (equal); methodology (equal); software (equal); supervision (equal); writing review and editing (equal). Susanna Asseyer: Data curation (equal); validation (equal); writing review and editing (equal). Joseph Kuchling: Data curation (equal); investigation (equal); supervision (equal); writing review and editing (equal). Judith Bellmann-Strobl: Data curation (equal); writing review and editing (equal). Klemens Ruprecht: Data curation (equal); investigation (equal); writing review and editing (equal). Maria Isabel Leite: Funding acquisition (equal); investigation (equal); supervision (equal); writing review and editing (equal). Friedemann Paul: Conceptualization (equal); funding acquisition (equal); investigation (equal); methodology (equal); project administration (equal); resources (equal); supervision (equal); writing review and editing (equal). Alexander U Brandt: Conceptualization (equal); data curation (equal); funding acquisition (equal); investigation (equal); methodology (equal); project administration (equal); resources (equal); supervision (equal); validation (equal); writing review and editing (equal). Jacqueline Palace: Conceptualization (equal); data curation (equal); funding acquisition (equal); investigation (equal); methodology (equal); project administration (equal); resources (equal); supervision (equal); validation (equal); writing review and editing (equal).

## ETHICAL APPROVAL

Patients were recruited and consented from ongoing cohort studies of patients with AQP4-Ab seropositive NMOSD at Oxford University Hospital (REC 16/SC/0224) and Charité – Universitätsmedizin Berlin (EA1/131/09). Healthy controls from the University of Oxford were

recruited under ethics 17/EE/0246 and EA1/182/10 at Charité – Universitätsmedizin Berlin. The study was conducted in accordance with the current version of the Declaration of Helsinki and the applicable British and German laws. All participants gave written informed consent.

## CONSENT FOR PUBLICATION

Consent for publication was included in consent forms submitted to ethics.

## DATA AVAILABILITY STATEMENT

The datasets during and/or analysed during the current study are available from the corresponding author on reasonable request.

## ORCID

Adriana Roca-Fernández  <https://orcid.org/0000-0002-8720-9397>

[org/0000-0002-8720-9397](https://orcid.org/0000-0002-8720-9397)

Jaume Sastre-Garriga  <https://orcid.org/0000-0002-1589-2254>

Susanna Asseyer  <https://orcid.org/0000-0001-6289-1791>

## REFERENCES

- Pittock SJ, Lucchinetti CF. Neuromyelitis optica and the evolving spectrum of autoimmune aquaporin-4 channelopathies: a decade later. *Ann N Y Acad Sci*. 2016;1366(1):20-39.
- Lennon VA, Wingerchuk DM, Kryzer TJ, et al. A serum autoantibody marker of neuromyelitis optica: distinction from multiple sclerosis. *Lancet Lond Engl*. 2004;364(9451):2106-2112.
- Zekeridou A, Lennon VA. Aquaporin-4 autoimmunity. *Neurol Neuroimmunol Neuroinflammation*. 2015;2(4):e110.
- Waters P, Jarius S, Littleton E, et al. Aquaporin-4 antibodies in neuromyelitis optica and longitudinally extensive transverse myelitis. *Arch Neurol*. 2008;65(7):913-919.
- Wingerchuk DM, Pittock SJ, Lucchinetti CF, Lennon VA, Weinshenker BG. A secondary progressive clinical course is uncommon in neuromyelitis optica. *Neurology*. 2007;68(8):603-605.
- Schmidt F, Zimmermann H, Mikolajczak J, et al. Severe structural and functional visual system damage leads to profound loss of vision-related quality of life in patients with neuromyelitis optica spectrum disorders. *Mult Scler Relat Disord*. 2017;11:45-50.
- Hokari M, Yokoseki A, Arakawa M, et al. Clinicopathological features in anterior visual pathway in neuromyelitis optica. *Ann Neurol*. 2016;79(4):605-624.
- Oertel FC, Zimmermann H, Paul F, Brandt AU. Optical coherence tomography in neuromyelitis optica spectrum disorders: potential advantages for individualized monitoring of progression and therapy. *EPMA J*. 2017;9(1):21-33.
- Oertel FC, Kuchling J, Zimmermann H, et al. Microstructural visual system changes in AQP4-antibody-seropositive NMOSD. *Neurol Neuroimmunol Neuroinflammation [Internet]*. 2017;4(3):e334.
- Oertel FC, Havla J, Roca-Fernández A, et al. Retinal ganglion cell loss in neuromyelitis optica: a longitudinal study. *J Neurol Neurosurg Psychiatry*. 2018;89(12):1259-1265.
- Jeong IH, Kim HJ, Kim N-H, Jeong KS, Park CY. Subclinical primary retinal pathology in neuromyelitis optica spectrum disorder. *J Neurol*. 2016;263(7):1343-1348.
- Felix CM, Levin MH, Verkman AS. Complement-independent retinal pathology produced by intravitreal injection of neuromyelitis optica immunoglobulin G. *J Neuroinflammation*. 2016;13(1):275.

13. Bringmann A, Pannicke T, Grosche J, et al. Müller cells in the healthy and diseased retina. *Prog Retin Eye Res.* 2006;25(4):397-424.
14. Bringmann A, Reichenbach A, Wiedemann P. Pathomechanisms of cystoid macular edema. - PubMed - NCBI [Internet]. [cited 2019 Oct 21]. <https://www.ncbi.nlm.nih.gov/pubmed/15583429>.
15. Goodyear MJ, Crewther SG, Junghans BM. A role for aquaporin-4 in fluid regulation in the inner retina. *Vis Neurosci.* 2009;26(2):159-165.
16. Nishikawa S, Tamai M. Müller cells in the human foveal region. *Curr Eye Res.* 2001;22(1):34-41.
17. Yadav SK, Motamedi S, Oberwahrenbrock T, et al. CuBe: parametric modeling of 3D foveal shape using cubic Bézier. *Biomed Opt Express.* 2017;8(9):4181-4199.
18. Motamedi S, Oertel FC, Yadav SK, et al. Altered fovea in AQP4-IgG-seropositive neuromyelitis optica spectrum disorders. *Neurol Neuroimmunol Neuroinflammation.* 2020;7(5):e805.
19. Wingerchuk DM, Banwell B, Bennett JL, et al. International consensus diagnostic criteria for neuromyelitis optica spectrum disorders. *Neurology.* 2015;85(2):177-189.
20. Tewarie P, Balk L, Costello F, et al. The OSCAR-IB consensus criteria for retinal OCT quality assessment. *PLoS One.* 2012;7(4):e34823.
21. Cruz-Herranz A, Balk LJ, Oberwahrenbrock T, et al. The APOSTEL recommendations for reporting quantitative optical coherence tomography studies. *Neurology.* 2016;86(24):2303-2309.
22. Worley B, Powers R. PCA as a Practical Indicator of OPLS-DA Model Reliability [Internet]. 2016 [cited 2019 Oct 21]. <https://www.ingen-taconnect.com/content/ben/cmb/2016/00000004/00000002/art00004>.
23. Jurynczyk M, Probert F, Yeo T, et al. Metabolomics reveals distinct, antibody-independent, molecular signatures of MS, AQP4-antibody and MOG-antibody disease. *Acta Neuropathol Commun.* 2017;5(1):95.
24. Yeo T, Probert F, Jurynczyk M, et al. Classifying the antibody-negative NMO syndromes: clinical, imaging, and metabolomic modeling. *Neurol Neuroimmunol Neuroinflammation.* 2019;6(6):e626.
25. Thévenot EA, Roux A, Xu Y, Ezan E, Junot C. Analysis of the human adult urinary metabolome variations with age, body mass index, and gender by implementing a comprehensive workflow for univariate and OPLS statistical analyses. *J Proteome Res.* 2015;14(8):3322-3335.
26. Pisa M, Ratti F, Vabanesi M, et al. Subclinical neurodegeneration in multiple sclerosis and neuromyelitis optica spectrum disorder revealed by optical coherence tomography. *Mult Scler J.* 2019;26(10):1197-1206.
27. Pache F, Zimmermann H, Mikolajczak J, et al. MOG-IgG in NMO and related disorders: a multicenter study of 50 patients. Part 4: Afferent visual system damage after optic neuritis in MOG-IgG-seropositive versus AQP4-IgG-seropositive patients. *J Neuroinflammation.* 2016;13(1):282.
28. Ramanathan S, Prelog K, Barnes EH, et al. Radiological differentiation of optic neuritis with myelin oligodendrocyte glycoprotein antibodies, aquaporin-4 antibodies, and multiple sclerosis. *Mult Scler J.* 2016;22(4):470-482.
29. Petzold A, Wattjes MP, Costello F, et al. The investigation of acute optic neuritis: a review and proposed protocol. *Nat Rev Neurol.* 2014;10(8):447-458.
30. Gleiser C, Wagner A, Fallier-Becker P, Wolburg H, Hirt B, Mack AF. Aquaporin-4 in astroglial cells in the CNS and supporting cells of sensory organs—a comparative perspective. *Int J Mol Sci [Internet].* 2016;17(9):1411. <https://www.ncbi.nlm.nih.gov/pmc/articles/PMC5037691/>.
31. Bennett JL, Owens GP. Neuromyelitis optica: deciphering a complex immune-mediated astrocytopathy. *J Neuro-Ophthalmol Off J North Am Neuro-Ophthalmol Soc.* 2017;37(3):291-299.
32. Provis JM, Penfold PL, Cornish EE, Sandercoe TM, Madigan MC. Anatomy and development of the macula: specialisation and the vulnerability to macular degeneration. *Clin Exp Optom.* 2005;88(5):269-281.
33. Artal P. Image formation in the living human eye. *Annu Rev Vis Sci.* 2015;1:1-17.
34. Sotirchos ES, Filippatou A, Fitzgerald KC, et al. Aquaporin-4 IgG seropositivity is associated with worse visual outcomes after optic neuritis than MOG-IgG seropositivity and multiple sclerosis, independent of macular ganglion cell layer thinning. *Mult Scler J [Internet].* 2020. 26(11):1360-1371. <https://journals.sagepub.com/doi/10.1177/1352458519864928>.
35. Oertel FC, Schließeit J, Brandt AU, Paul F. Cognitive impairment in neuromyelitis optica spectrum disorders: a review of clinical and neuroradiological features. *Front Neurol [Internet].* 2019. 10. <https://doi.org/10.3389/fneur.2019.00608>.
36. Penner I-K, Paul F. Fatigue as a symptom or comorbidity of neurological diseases. *Nat Rev Neurol.* 2017;13(11):662-675.
37. Asseger S, Schmidt F, Chien C, et al. Pain in AQP4-IgG-positive and MOG-IgG-positive neuromyelitis optica spectrum disorders. *Mult Scler J Exp Transl Clin.* 2018;4(3). <https://doi.org/10.1177/2055217318796684>.
38. Chavarro VS, Mealy MA, Simpson A, et al. Insufficient treatment of severe depression in neuromyelitis optica spectrum disorder. *Neurol Neuroimmunol Neuroinflammation [Internet].* 2016;3(6):e286. <https://www.ncbi.nlm.nih.gov/pmc/articles/PMC5079380/>.
39. Liu Y, Duan Y, He Y, et al. A tract-based diffusion study of cerebral white matter in neuromyelitis optica reveals widespread pathological alterations. *Mult Scler J.* 2012;18(7):1013-1021.
40. Finke C, Zimmermann H, Pache F, et al. Association of visual impairment in neuromyelitis optica spectrum disorder with visual network reorganization. *JAMA Neurol.* 2018;75(3):296-303.
41. Papadopoulou A, Oertel FC, Gaetano L, et al. Attack-related damage of thalamic nuclei in neuromyelitis optica spectrum disorders. *J Neurol Neurosurg Psychiatry.* 2019;90(10):1156-1164.
42. Xiao M, Hu G. Involvement of aquaporin 4 in astrocyte function and neuropsychiatric disorders. *CNS Neurosci Ther.* 2014;20(5):385-390.
43. Ringelstein M, Harmel J, Zimmermann H, et al. Longitudinal optic neuritis-unrelated visual evoked potential changes in NMO spectrum disorders. *Neurology.* 2020;94(4):e407-e418.

**How to cite this article:** Roca-Fernández A, Oertel FC, Yeo T, et al. Foveal changes in aquaporin-4 antibody seropositive neuromyelitis optica spectrum disorder are independent of optic neuritis and not overtly progressive. *Eur J Neurol.* 2021;28:2280-2293. <https://doi.org/10.1111/ene.14766>

## APPENDIX A

### FOVEA MORPHOMETRY

The fovea morphometry method is described in detail by Yadav et al. [17]. Fovea morphometry characterizes the foveal and parafoveal region by 19 parameters. The method first flattens the inner limiting membrane (ILM) surface according to Bruch's membrane as the reference (reference plane) and then radially reconstructs the ILM surface, from the centre of the fovea up to the points with maximum heights which are called rim points, using cubic Bézier polynomials. Based on the reconstructed ILM surface and the reference plane, foveal morphometry parameters are defined. Twelve parameters are defined as area, average diameter, major length (the length in the dominant direction) and minor length (the length in the second dominant direction,

perpendicular to the dominant direction) of three different surfaces: pit flat disc, a surface that captures the flatness of the foveal pit; slope disc, a surface that connects points with maximum slope; and rim disc, a surface that connects rim points. In addition to the parameters describing the defined surfaces, there are several other parameters describing the fovea: average pit depth, average height of the points on the pit flat disc; central foveal thickness, minimum thickness of the

fovea; average rim height, average height of rim points; rim volume, volume between the ILM surface and the reference plane limited to rim points; inner rim volume, similar to rim volume but limited to 1-mm diameter around the centre of the fovea; pit volume, volume between the ILM surface and the rim disc; and average maximum pit slope, average slope of points with maximum slope. Figure A1 shows an overview of the fovea morphometry method.

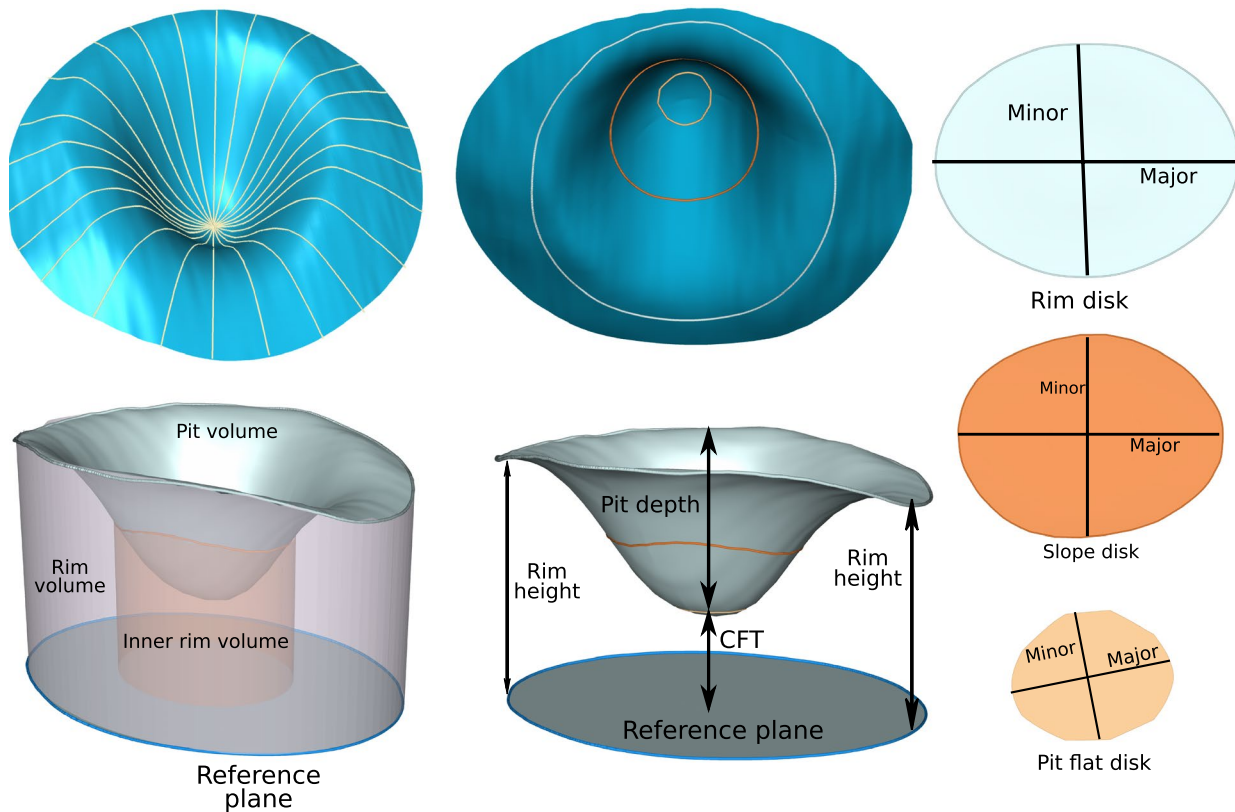


**FIGURE A1** 3D representation of the foveal shape. [Colour figure can be viewed at [wileyonlinelibrary.com](http://wileyonlinelibrary.com)]



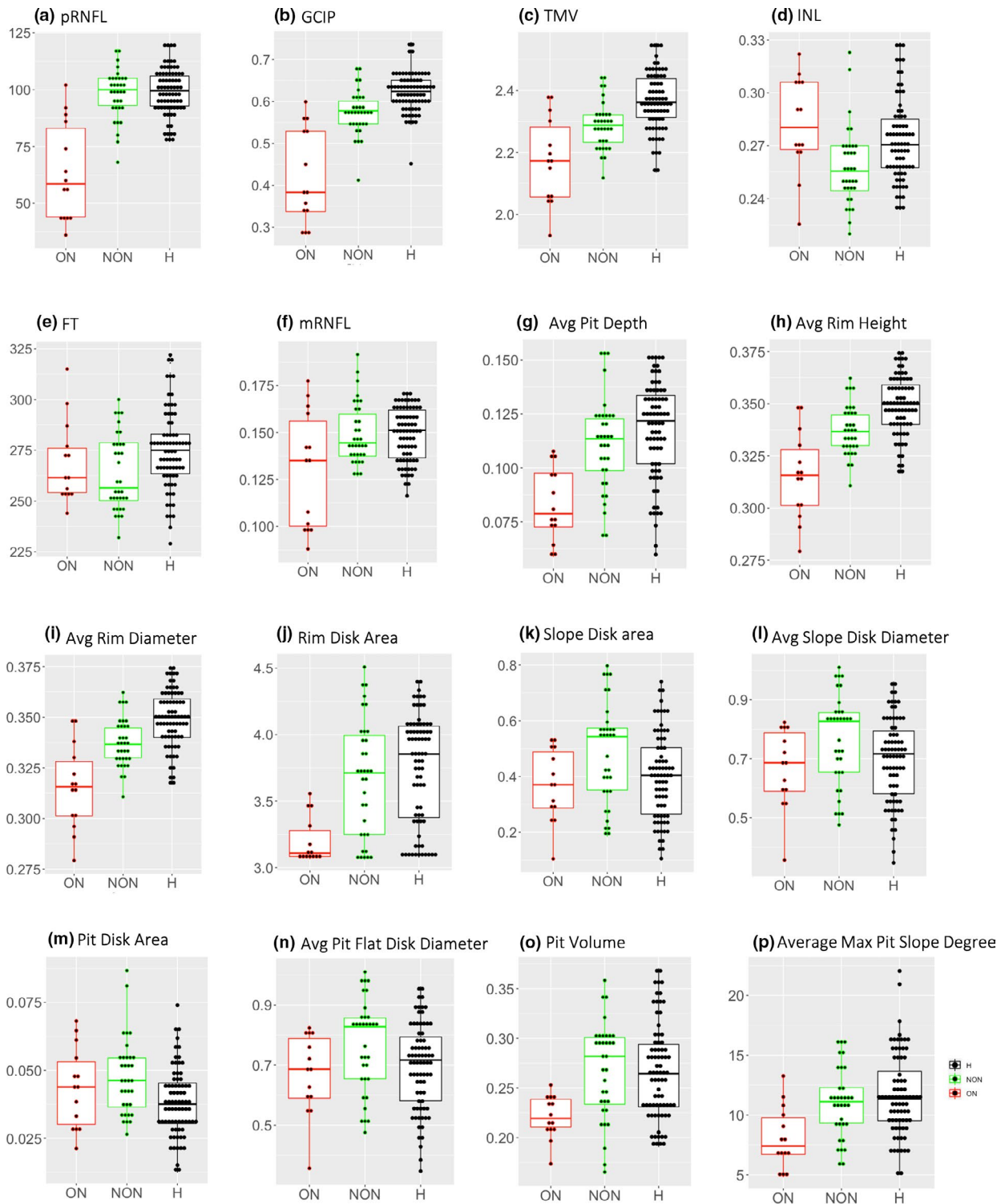


**FIGURE A2** Box plots of disc and macular baseline OCT and foveal data where there are significant differences between at least one group: (a) peripapillary retinal nerve fibre layer (pRNFL) at the disc; (b) combined ganglion cell and inner plexiform layer volume (GCIP); (c) total macular volume (TMV); (d) inner nuclear layer (INL); (e) foveal thickness (FT); (f) retinal nerve fibre layer at the macula (mRNFL); (g) average pit depth; (h) average rim height; (i) average rim diameter; (j) rim disc area; (k) slope disc area; (l) average slope disc diameter; (m) pit disc area; (n) average pit flat disc diameter; (o) pit volume; (p) average maximum pit slope degree. The boxplots show the median and 25th and 75th percentiles [Colour figure can be viewed at [wileyonlinelibrary.com](http://wileyonlinelibrary.com)]